Nature and Science of Sleep

Elevate Series

Open Access Full Text Article

ORIGINAL RESEARCH

White Matter Imaging Phenotypes Mediate the Negative Causality of Mitochondrial DNA Copy Number on Sleep Apnea: A Bidirectional Mendelian Randomization Study and Mediation Analysis

Qiaohui Ying[1–4,*], Mingwei Wang[5,*], Zichen Zhao[1–4], Yongwei Wu[1–4], Changyun Sun[1–4], Xinyi Huang[1–4], Xin Zhang[1–4], Jie Guo[1–4]

[1]Department of Orthodontics, School and Hospital of Stomatology, Cheeloo College of Medicine, Shandong University, Jinan, Shandong, People's Republic of China; [2]Shandong Key Laboratory of Oral Tissue Regeneration, Shandong University, Jinan, Shandong, People's Republic of China; [3]Shandong Engineering Research Center of Dental Materials and Oral Tissue Regeneration, Shandong University, Jinan, Shandong, People's Republic of China; [4]Shandong Provincial Clinical Research Center for Oral Diseases, Shandong University, Jinan, Shandong, People's Republic of China; [5]Institute of Blood Transfusion, Chinese Academy of Medical Sciences and Peking Union Medical College, Chengdu, Sichuan, Republic of China.

*These authors contributed equally to this work

Correspondence: Jie Guo, Department of Orthodontics, School and Hospital of Stomatology, Shandong University, No. 44-1 Wenhua Road West, Jinan, Shandong, 250012, People's Republic of China, Tel +86 13583104999, Fax +86 53188382923, Email kqgj@sdu.edu.cn

Video abstract

Point your SmartPhone at the code above. If you have a QR code reader the video abstract will appear. Or use: https://youtu.be/L82ERJH0E7w

Purpose: Sleep apnea (SA), associated with absent neural output, is characterised by recurrent episodes of hypoxemia and repeated arousals during sleep, resulting in decreased sleep quality and various health complications. Mitochondrial DNA copy number (mtDNA-CN), an easily accessible biomarker in blood, reflects mitochondrial function. However, the causal relationship between mtDNA-CN and SA remains unclear. This study aimed to investigate the causality between mtDNA-CN and SA while identifying potential mediating brain imaging phenotypes (BIPs).

Methods: Two-sample bidirectional Mendelian randomisation (MR) analysis was performed to estimate the causal relationship between mtDNA-CN and SA, with further validation using Bayesian framework-based MR analysis. A two-step approach was employed to evaluate causal relationships between BIPs, mtDNA-CN and SA, utilising the "product of coefficients" method to assess the mediating effects of BIPs. Multiple testing errors were corrected using the Benjamini–Hochberg method.

Results: Genetically predicted mtDNA-CN had a negative causal effect on SA (OR = 0.859, 95% CI = 0.785–0.939, $P = 3.20\times10^{-4}$), whereas SA did not have a causal effect on mtDNA-CN (OR = 1.0056, 95% CI = 0.9954–1.0159, $P = 0.2825$). Among 3935 BIPs, two features related to white matter microstructure served as partial mediators: the second eigenvalue from diffusion MRI data analysed by tract-based spatial statistics in the right posterior thalamic radiation, with a mediation proportion of 11.37% ($P = 0.0450$), and fractional anisotropy in the right sagittal stratum, with a mediation proportion of 12.79% ($P = 0.0323$).

Conclusion: This study demonstrated a causal relationship between mtDNA-CN and SA, with specific brain white matter microstructure phenotypes potentially acting as mediators. These findings highlight the potential of mtDNA-CN as a biomarker for SA and underscore its relevance in guiding future therapeutic strategies targeting mitochondrial health and brain white matter microstructure.

Keywords: mitochondrion, sleep disorder, brain structure, magnetic resonance imaging, causal relationship

Introduction

Sleep apnea (SA), characterised by recurrent pharyngeal collapse during sleep leading to apnoea and hypopnea, results in hypoxemia, hypercapnia, and repeated arousals.[1] Studies have indicated that both central and obstructive SA involve reduced or absent neural output from the brain to the upper airway muscles and/or lower thoracic inspiratory pump muscles.[2] This condition affects more than 900 million people worldwide, with approximately 40% experiencing

Received: 19 July 2024
Accepted: 26 November 2024
Published: 17 December 2024

moderate to severe disease and the highest number of affected individuals observed in China (more than 744 million).[3] It is also a risk factor for numerous diseases, including craniofacial deformity, stroke, diabetes, cardiovascular diseases, and cancer.[4–6] Current interventions, such as positive airway pressure therapy, orthodontic treatments, and airway and jaw surgeries, are typically initiated only after severe symptoms or complications arise and have not been shown to reduce cardiovascular events or mortality rates.[7] This underscores the need for further etiological research, genetic exploration, and clinical prediction in SA progression.

Mitochondria, often referred to as the cell's oxygen-processing factories, play essential roles in energy metabolism and organ function. It contains its own circular DNA (mtDNA), whose copy number (mtDNA-CN) partially reflects mitochondrial quantity and quality.[8,9] This indicator, easily estimated from whole blood, serves as a potential marker of metabolic health across multiple organ systems and thus may hold promise as a clinical predictive tool.[10] However, its relationship with SA remains unclear. Recent studies indicate a higher prevalence of sleep-disordered breathing in individuals with mitochondrial diseases,[11] while a small clinical study by Yoo-Suk K et al suggested mtDNA-CN as a possible marker of oxidative stress in SA patients.[12] Biologically, mtDNA-CN could influence SA through mechanisms involving neural transmission and airway inflammation, while SA may also affect mtDNA-CN by altering mitochondrial function.[13–15] Thus, further investigation into the causal relationship between mtDNA-CN and SA is essential to elucidate underlying mechanisms and identify predictive and therapeutic tools.

Brain structure characteristics are associated with the severity of SA and mitochondrial function. For instance, SA is associated with reduced tissue fractional anisotropy and smaller volumes in the fornix, potentially contributing to memory impairment in individuals with mild cognitive impairment.[16] Magnetic resonance imaging (MRI) indicators of the brain's perivascular space network exhibit differences among patients with varying severities of SA.[17] Recent studies have demonstrated associations between mtDNA-CN and brain MRI markers (eg, hippocampal volume and white matter hyperintensity) as well as cognitive function,[18] as well as correlations with symptoms and severity of neurological disorders, such as Alzheimer's disease, stroke, and schizophrenia.[18–20] Therefore, it is necessary to further explore the causal relationships between brain structure, mtDNA-CN, and SA in the context of genetic prediction to facilitate early diagnosis, risk stratification, and the development of targeted therapeutic strategies.

These unmet needs can be addressed by applying Mendelian randomisation (MR) analysis. MR offers a novel perspective for epidemiological research by utilising genetic variants as instrumental variables (IVs) to determine causal relationships between exposures and outcomes.[21] The random distribution of alleles at birth makes MR analogous to the principles of randomised controlled trials, thereby overcoming the limitations of traditional analyses in establishing causality and mitigating the impact of potential confounding factors on result accuracy.[22] Additionally, MR can enhance causal inference in mediation analysis, circumventing the need for assumptions about unmeasured confounding.[23] The latest MR studies on mtDNA-CN have investigated causal links with severe diseases such as stroke, cancer, and psychiatric disorders,[24–26] yet none have addressed sleep-related outcomes.

This study used genome-wide association study (GWAS) data and MR methods to evaluate the causal relationship between mtDNA-CN and SA. Given the close association between brain imaging phenotypes (BIPs) and SA, we also investigated whether these neurological markers mediated the effect of mtDNA-CN on SA risk.

Materials and Methods

Research Description

The data used in this study included publicly accessible summary-level data. Figure 1 illustrates the framework of the experimental design. Initially, a two-sample MR analysis was performed to investigate the causal relationship between mtDNA-CN and SA. Subsequently, a two-step MR analysis was conducted to identify BIPs that might act as mediators. Bayesian framework-based MR (BFMR) analysis was employed throughout these processes to further support the former results. Additionally, the MR design had to meet three core assumptions: relevance, independence, and exclusion restriction.[27] This study adhered to the guidelines established by the *Strengthening the Reporting of Observational Studies in Epidemiology using Mendelian Randomization* (STROBE-MR) guideline (Table S1).[28]

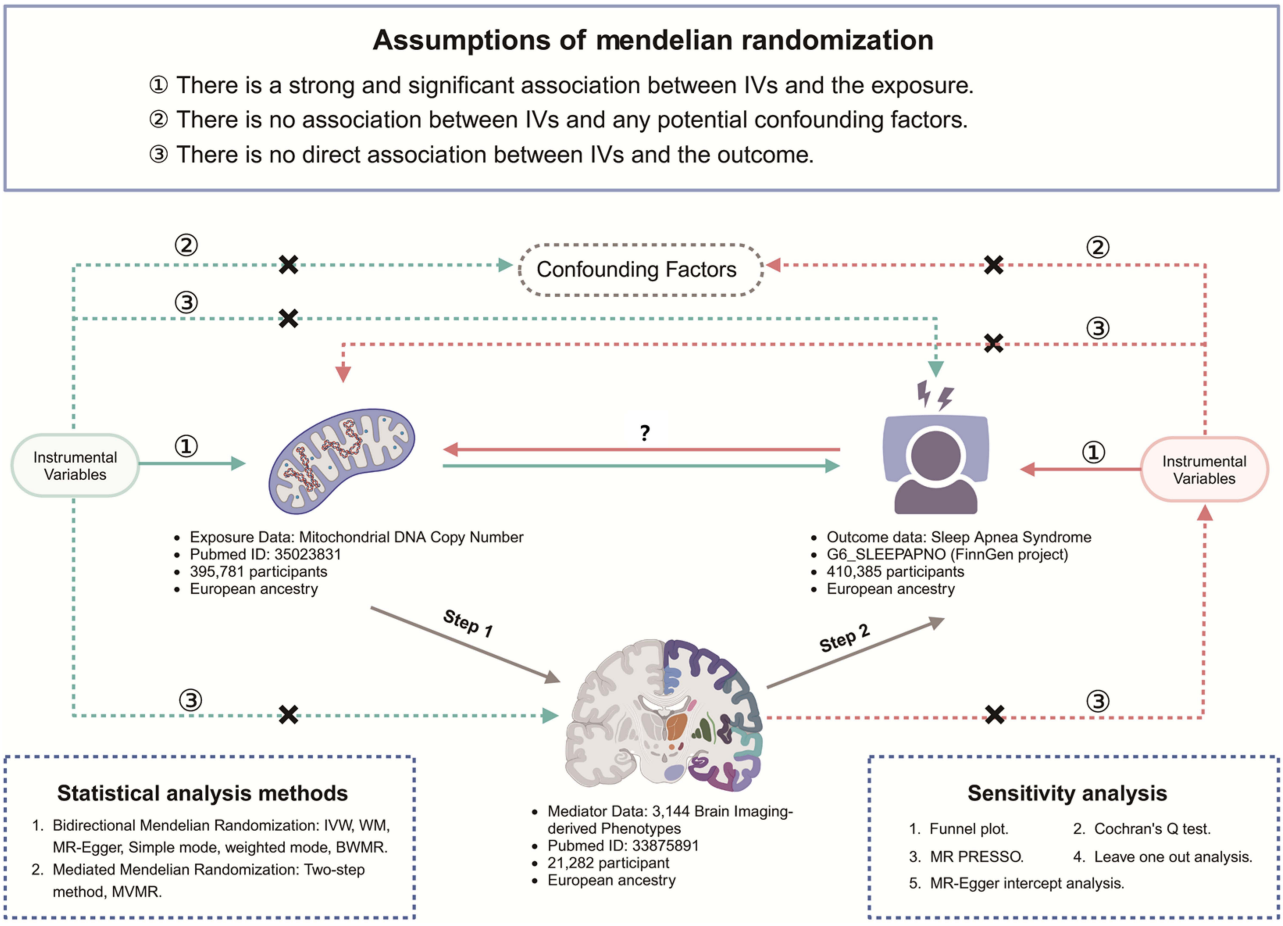

Figure 1 Schematic diagram of the study design. This diagram includes the three assumptions of MR, the process of two-step MR, the data analysis methods, the sensitivity analysis approaches. Green arrows represent forward MR analyses, with blood mtDNA-CN as the exposure and SA as the outcome; red arrows represent reverse MR analyses, with SA as the exposure and blood mtDNA-CN as the outcome. Solid lines indicate components that meet MR assumptions, while dashed lines represent those that do not satisfy MR assumptions. This figure was created using BioRender.com.

Data Sources

The exposure data for mtDNA-CN was derived from the study by Michael C et al, which reported polygenic low mtDNA-CN variation in the blood of 395,781 European individuals from the UK Biobank (2006 to 2010).[29] This study indicated that mtDNA-CN differences primarily reflect mitochondrial processes associated with dNTP metabolism and the replication, maintenance and development of the "AutoMitoC" method. The outcome data for SA patients were obtained from the FinnGen database (G6_SLEEPAPNO), which includes information from 43,901 SA patients and 366,484 controls. The FinnGen project is a major genomics initiative analysing genetic data from over 500,000 Finnish biobank samples to uncover disease mechanisms involving collaboration between Finnish research institutions, biobanks, and international partners.[30] The GWAS data for 3144 BIPs were derived from the study by Stephen MS et al, which utilized brain imaging data from 33,224 participants released in early 2020 in the UK.[31] The naming system used in this study is derived from Imaging-Derived Phenotypes (IDPs). The characteristics of the GWAS summary-level data, which were authorized and ethically approved by the original studies, are listed in Table S2.

Partial Interpretation of BIPs Naming Rules Based on IDPs

Physiological changes in the brain can be non-invasively measured using MRI.[32] Brain connectivity can be divided into functional connectivity, where spontaneous temporal synchronizations between brain regions are measured using functional MRI (fMRI) with subjects scanned at rest, and structural connectivity, measured using diffusion MRI (dMRI), which images the physical connections between brain regions based on how water molecules diffuse within white matter

tracts. Tract-Based Spatial Statistics (TBSS) enables whole-brain analysis of white matter skeletons. In dMRI, commonly used indices include fractional anisotropy (FA) and the second eigenvalue of the diffusion tensor (L2). In contrast to other white matter imaging measures, a low FA signal typically indicates reduced white matter integrity, while a low L2 signal suggests improved white matter coherence and structural preservation.[33]

IVs and Data Harmonisation

In this study, a relatively permissive significance threshold ($P < 1\times10^{-5}$) was adopted for instrumental variable (IV) selection to include as many SNPs as possible.[34] When the number of SNPs was relatively large, a stricter threshold ($P < 5\times10^{-8}$) was applied to validate the accuracy of the results. Subsequently, instruments were pruned based on a linkage disequilibrium (LD) threshold using PLINK, with $r^2 < 0.001$ and a distance > 10000 kb, retaining the SNPs with the lowest P values. Potential confounders, such as obesity and age, were removed using LDLink (https://github.com/CBIIT/LDlinkR). Palindromic SNPs and SNPs associated with the outcome ($P < 1\times10^{-5}$) were excluded, and SNPs with a minor allele frequency of 0.01 or lower were omitted to ensure robustness.[35] The F-statistics for individual SNPs $\left(F = \frac{R^2*(n-2)}{(1-R^2)*n}\right)$ were calculated. Subsequently, the overall F-statistic for the instrument set $\left(F = \frac{R_{overall}\hat{2}\times(N-K-1)}{\left(1-R^2_{overall}\right)\times K}\right)$, where "N" is the sample size, "K" is the number of instruments.[36] SNPs with an F-statistic below the conventional threshold of 10 were excluded to mitigate weak instrument bias.[37] SNPs with F-statistics in the range of 10–20 were considered borderline and were excluded for re-evaluation of the results.

Statistical Analysis

Univariate Mendelian Randomization Analysis

The inverse variance weighted (IVW) method was mainly employed to assess causal relationships, as it is deemed reliable in the absence of directional pleiotropy.[38] Other analytical methods, such as MR Egger, weighted median, simple mode and weighted mode, were used for reference. Scatter plots were utilized to depict causal directions, while forest plots showed effect sizes and their statistical significance. The analysis was conducted using R version 4.4.0 and the TwoSampleMR package (https://mrcieu.github.io/TwoSampleMR/articles/introduction.html).[39] Specific functions from this package supported the MR analysis, ensuring robust and replicable outcomes.

MR Analysis for Mediation

Through two-step MR analysis, we explored the potential mediating role of BIPs in the relationship between mtDNA-CN and SA. The mediation effect was evaluated using the product of coefficients method, where Step 1 estimated the effect of the genetic instrument on the BIPs (βXZ), and Step 2 estimated the effect of the BIPs on SA (βZY). Both steps primarily employed the IVW method, similar to the approach described in Univariate Mendelian Randomization Analysis. The mediation proportion of each BIP in the association between mtDNA-CN and SA was calculated as the product of βXZ and βZY divided by the total effect of mtDNA-CN on SA. The 95% confidence intervals (CIs) for the mediation proportion were computed using the delta method.[40,41]

BFMR Analysis

Considering the increased potential for bias due to invalid instruments with the addition of more instrumental variables, this study employs a Bayesian framework-based MR analysis for IVW significant or deemed significant results to enhance the robustness of the findings. This analytical method was recently proposed by Andrew JG et al.[42] This Bayesian framework provides practical causal inference under very general settings, accounting for both related and unrelated pleiotropy. Even in high pleiotropy scenarios, this method maintains the Type I error rate below the nominal level. The "mrhorse" package used in this study is available at https://github.com/aj-grant/mrhorse.

Multiple Testing Correction

FDR correction was performed using the Benjamini–Hochberg (BH) method.[43] The effective threshold (P') was recalculated for each stage based on the number of univariable MR analyses conducted in different directions: $P' = \frac{i}{m}a$, where "i" is the rank position of the P value, "m" is the total number of tests, and "α" is the predetermined significance level (α =

0.05). Associations with *P*-values less than 0.05 are not significant; *P*-values less than 0.05 but greater than P' are considered nominally significant, while those with P-values less than *P'* are deemed significant.

Sensitivity Analysis

We employed MR–Egger, weighted median, simple mode, and weighted mode methods for sensitivity analyses. The MR-Egger method examines the presence of directional pleiotropy based on its intercept, where a value significantly different from zero indicates directional pleiotropy and biased IVW estimates.[39] The results are considered robust if the direction of the estimates from these four methods aligns with those from IVW. Additionally, the Mendelian randomization pleiotropy residual sum and outlier (MR-PRESSO) method (https://github.com/rondolab/MR-PRESSO) was used to detect potential outliers and to re-estimate the causal effect after outlier removal to ascertain the presence of directional pleiotropy.[44] The MR-PRESSO method calculates the residual sum of squares observed (RSSobs), a measure that quantifies the extent of heterogeneity due to pleiotropy in the instrumental variables. If pleiotropy was detected, we reconducted the MR analysis after removing the outliers until no outliers were present. Cochrane's Q statistic was used to assess heterogeneity among instruments, and I^2 values <25%, 25–75% and >75% were considered to indicate low, moderate and high heterogeneity, respectively.[45]

Results

The Bidirectional Causal Relationship Between mtDNA-CN and SA

Detailed information about the IVs is provided in Table S3-4. The tables indicated that all selected IVs met the three core assumptions of MR. Initially, we performed bidirectional MR analysis to examine the causal relationship between mtDNA-CN and SA, utilizing 132 SNPs for mtDNA-CN and 140 SNPs for SA. Notably, the F-statistics for all individual SNPs and the combined IVs consistently exceeded 10.

The Causal Effect of mtDNA-CN on SA

In the analysis of causal effects between mtDNA-CN and SA, blood mtDNA-CN levels served as the exposure, while SA was the outcome. The overall F-statistic for the IVs was calculated to be 56.761 (Table S3). Results showed a significant negative correlation between mtDNA-CN and SA. The IVW method estimated that each standard deviation increase in mtDNA-CN corresponded to a decreased risk of SA, with an odds ratio (OR) of 0.8595 (95% CI [0.788, 0.937], P = 5.863×10^{-4}) (Figure 2A). The IVW forest plot supported this association across individual SNPs (Figure 2B). Although *P* values for the other methods were above 0.05, the IVW result was considered decisive in suggesting a causal link between mtDNA-CN and SA. Furthermore, the BFMR analysis corroborated the findings of the IVW method, producing a point estimate of −0.155 (Rhat = 1.002, 95% CI [−0.241, −0.071], $P = 3.13 \times 10^{-4}$) with evidence of convergence (Figure S1A-B). To confirm the robustness of the IVW result, additional methods (MR-Egger, MR-PRESSO, Q-statistic IVW) were used to check for pleiotropy and heterogeneity. The MR-Egger intercept (Egger intercept = 6.448×10^{-4}, *P* = 0.742) was close to zero (Figure 2C), MR-PRESSO indicated no confounding (RSSobs = 156.487, *P* = 0.08), and Q-statistic IVW (Cochran's Q = 153.814, I^2 = 14.8%, P = 0.085) showed no heterogeneity. The funnel plot indicated no bias in IV selection (Figure 2D). Leave-one-out analysis confirmed that no single SNP significantly influenced the mtDNA-CN effect estimate, reinforcing the observed association (Figure 2E). When the threshold of $P<5\times10^{-8}$ was applied for revalidation, the results remained consistent (Figure S2A-E). After removing marginal SNPs with individual F-statistics between 10 and 20, the calculations were repeated, and the results remained stable (Table S5). Together, these findings support a negative causal role for mtDNA-CN in reducing SA risk.

The Causal Effect of SA on mtDNA-CN

The overall F-statistic for the IVs of SA was calculated to be 25.648 (Table S4). The reverse MR analysis found no evidence of a causal relationship between SA and mtDNA-CN (OR = 1.004, 95% CI [0.995, 1.013], P = 0.403) (Figure 3A-B). BFMR analysis supported this null finding (Estimate = 0.005, 95% CI [−0.005, 0.017], P = 0.405). Sensitivity analyses indicated no horizontal pleiotropy (MR-Egger intercept = 5.173×10^{-4}, *P* = 0.563) (Figure 3C) or significant confounding (MR-PRESSO's RSSobs = 152.268, *P* = 0.231). Additionally, Q-statistic IVW (Cochran's Q = 150.264, I^2 = 7.5%, *P* = 0.471) and funnel plots (Figure 3D) showed low heterogeneity and no major bias among IVs.

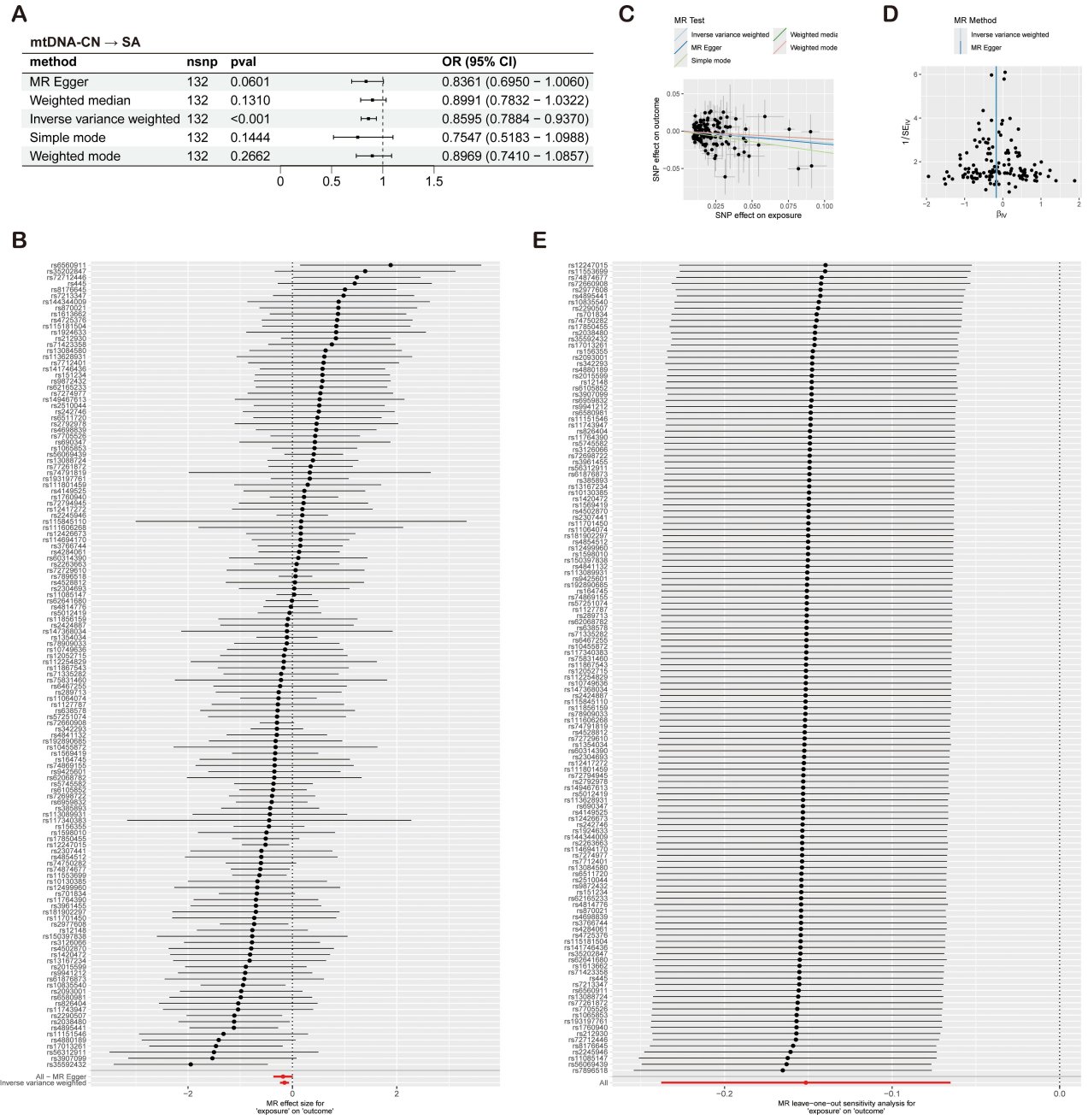

Figure 2 Forward causal analysis between mtDNA-CN (exposure) and SA (outcome). (**A**) The forest plot presented results from five MR methods. "nsnp" indicated the number of SNPs, "pval" represented the P-value, "OR" denoted the odds ratio, and "CI" indicated the confidence interval. (**B**) The forest plot showed individual SNP effects and the directions from MR-Egger and IVW. (**C**) The scatter plot illustrated the directions and intercepts, (**D**) The funnel plot assessed potential pleiotropy. (**E**) Leave-one-out analysis evaluated the robustness of the results.

Leave-one-out analysis further confirmed the stability of these findings, with no single SNP substantially affecting the association (Figure 3E). The results remained consistent when revalidation was conducted using a threshold of $P<5\times10^{-8}$ (Figure S3A-E). The calculations were repeated after excluding marginal SNPs with individual F-statistics ranging from 10 to 20, and the results remained consistent (Table S6).

MR Analysis of mtDNA-CN, BIPs and SA

Given the strong association between brain structure, mtDNA-CN and SA, we hypothesized that BIPs mediated the effect of mtDNA-CN on SA risk. A two-step MR mediation analysis was conducted, which ultimately identified two BIPs with potential mediating effects.

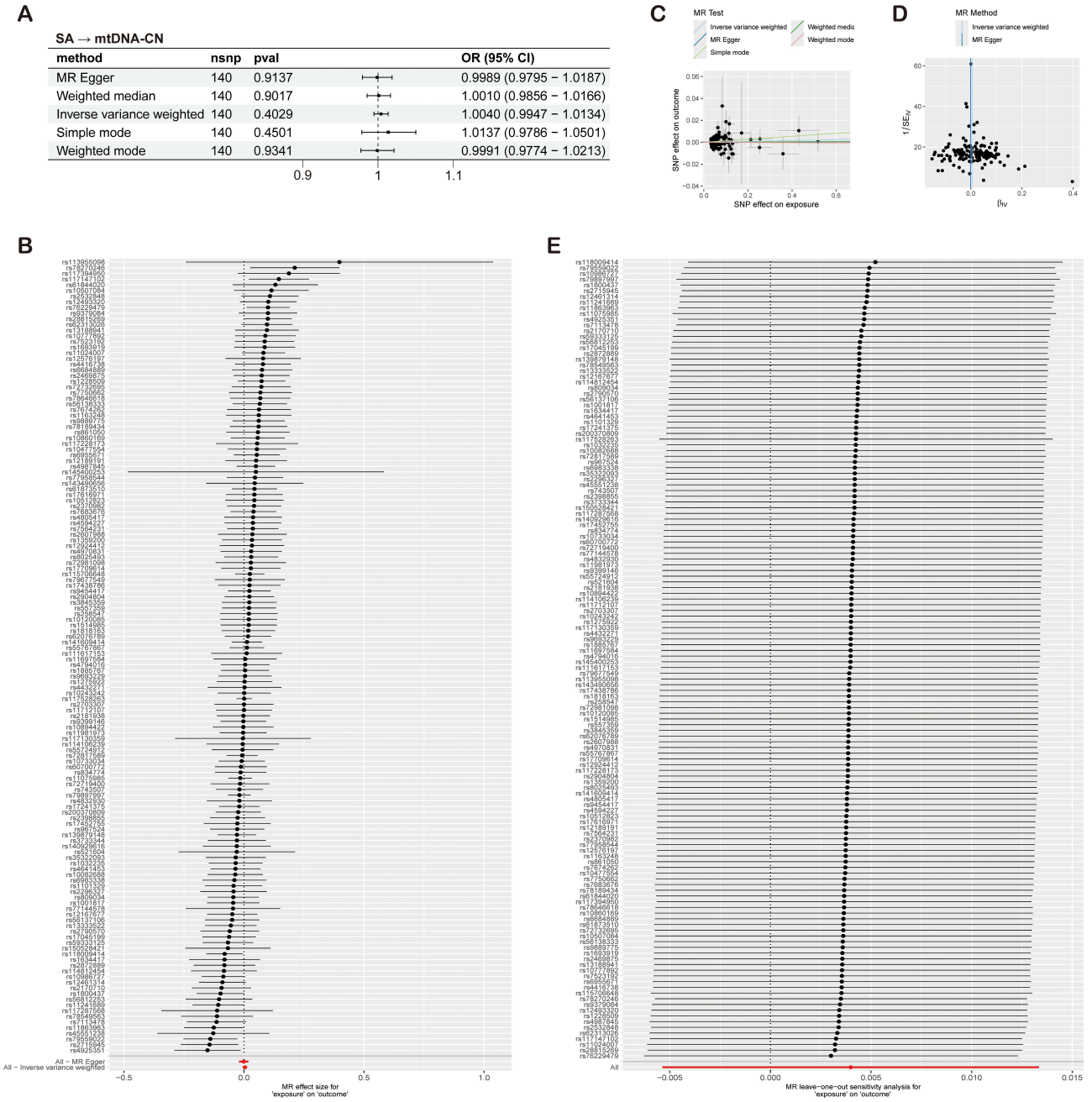

Figure 3 The reverse causal inference analysis examined blood mtDNA-CN as the outcome and SA as the exposure. (**A**) The forest plot presented the results of five MR analyses. "nsnp" indicated the number of single nucleotide polymorphisms, "pval" represented the P-value, "OR" denoted the odds ratio, and "CI" indicated the confidence interval. **(B)** The forest plot showed the effects of individual SNPs and the directions derived from IVW and MR-Egger. **(C)** The scatter plot illustrated the directions and intercepts. **(D)** The funnel plot assessed potential pleiotropy. **(E)** The leave-one-out analysis evaluated the robustness of the results.

The Causal Effect of mtDNA-CN on BIPs

Step 1 included a total of 3144 analyses. The IVW analysis identified potential associations between mtDNA-CN and 58 BIPs. After BH correction, mtDNA-CN remained significantly associated with 7 BIPs, while 51 showed nominal significance, and the remaining BIPs were not significant (Table S7). A heatmap illustrated the top 19 BIPs, which included fourteen brain connectivity measurements, three white matter microstructure metrics, and two mean fractional anisotropy measurements (Figure 4A). Apart from "IDP dMRI TBSS L2 Sagittal stratum R" (MR-PRESSO's RSSobs = 160.216, P = 0.042), no significant heterogeneity or horizontal pleiotropy was observed during the data analysis (Table 1). Notably, the directions indicated by simple mode analyses for "IDP dMRI TBSS L2 Sagittal stratum R"

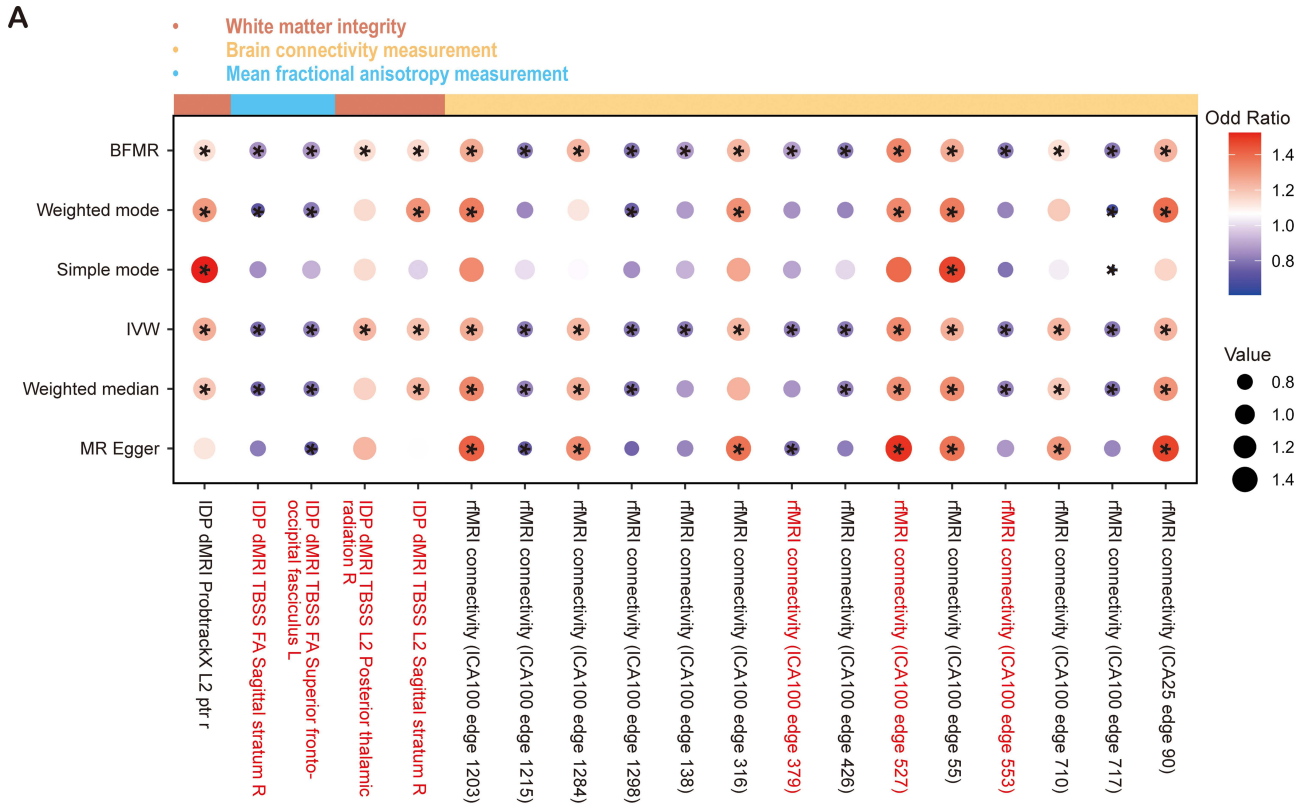

B

Traits	pval_1	OR_1 (95% CI)	pval_2	OR_2 (95% CI)
White matter integrity				
IDP dMRI ProbtrackX L2 ptr r	1.5615e−04	1.24 (1.11 to 1.39)	0.414905	0.98 (0.92 to 1.03)
* IDP dMRI TBSS L2 Posterior thalamic radiation R	2.6411e−04	1.23 (1.10 to 1.37)	0.000839	0.92 (0.88 to 0.97)
Mean fractional anisotrophy measurement				
* IDP dMRI TBSS FA Superior fronto−occipital fasciculus L	2.4948e−04	0.81 (0.73 to 0.91)	0.788963	0.99 (0.94 to 1.04)
* IDP dMRI TBSS FA Sagittal stratum R	2.3500e−05	0.78 (0.69 to 0.87)	0.000609	1.08 (1.03 to 1.13)
Brain connectivity measurement				
rfMRI connectivity (ICA100 edge 1203)	8.3428e−05	1.25 (1.12 to 1.40)	0.682745	1.02 (0.94 to 1.11)
rfMRI connectivity (ICA100 edge 1215)	1.6698e−04	0.81 (0.72 to 0.90)	0.998994	1.00 (0.91 to 1.10)
rfMRI connectivity (ICA100 edge 1284)	2.2762e−04	1.23 (1.10 to 1.36)	0.989711	1.00 (0.93 to 1.08)
rfMRI connectivity (ICA100 edge 1298)	8.6183e−05	0.80 (0.71 to 0.89)	0.160618	1.05 (0.98 to 1.13)
rfMRI connectivity (ICA100 edge 138)	1.6759e−04	0.81 (0.73 to 0.90)	0.837126	0.99 (0.92 to 1.07)
rfMRI connectivity (ICA100 edge 316)	2.3067e−04	1.23 (1.10 to 1.37)	0.526245	0.98 (0.92 to 1.04)
* rfMRI connectivity (ICA100 edge 379)	2.5595e−04	0.82 (0.73 to 0.91)	0.522237	0.98 (0.92 to 1.04)
rfMRI connectivity (ICA100 edge 426)	1.1530e−04	0.81 (0.73 to 0.90)	0.778859	1.01 (0.94 to 1.08)
* rfMRI connectivity (ICA100 edge 527)	1.0999e−06	1.33 (1.19 to 1.49)	0.653486	0.98 (0.91 to 1.06)
rfMRI connectivity (ICA100 edge 55)	1.1830e−04	1.24 (1.11 to 1.39)	0.401841	1.03 (0.95 to 1.12)
* rfMRI connectivity (ICA100 edge 553)	1.8779e−04	0.81 (0.72 to 0.90)	0.201910	0.96 (0.90 to 1.02)
rfMRI connectivity (ICA100 edge 710)	1.8226e−04	1.23 (1.10 to 1.37)	0.785135	0.99 (0.92 to 1.07)
rfMRI connectivity (ICA100 edge 717)	2.4068e−04	0.81 (0.72 to 0.90)	0.525157	1.01 (0.98 to 1.05)
rfMRI connectivity (ICA25 edge 90)	1.2104e−04	1.24 (1.11 to 1.38)	0.696192	1.02 (0.93 to 1.12)

Figure 4 Screening of BIPs related to mtDNA-CN and SA. **(A)** The heatmap showed the BIPs associated with mtDNA-CN after BH correction, with mtDNA-CN as the exposure and BIPs as the outcomes. * indicated $P < 0.05$. The red font indicated significant differences after multiple corrections. **(B)** The forest plot displayed the potential BIPs selected as mediators using the IVW method, highlighted in red. The columns with the suffix "1" indicated the specific results with mtDNA-CN as the exposure affecting BIPs, and the columns with the suffix "2" indicated the specific results with BIPs as the exposure affecting SA. * indicated significant differences after multiple corrections.

and "rfMRI connectivity (ICA100 edge 1215)" differed from those of the other methods, leading to their exclusion from further analysis (Table S8). Consequently, at this step, the causal relationships between mtDNA-CN and only 6 BIPs were considered significant. Forest plots and sensitivity analyses for these results were presented in Figure S4-9. The results remained consistent regardless of whether a threshold of $P<5\times10^{-8}$ was applied or borderline SNPs were excluded (Tables S9-11).

Table 1 Heterogeneity and Pleiotropy of the First-Step Results in Mendelian Randomization Mediation Analysis

Exposure	Outcome	Q in MR Egger	Q_pval in MR Egger[a]	Egger_intercept	pval	RSSobs[b]	Global Test P-value[c]
mtDNA-CN	rfMRI connectivity (ICA100 edge 527)	106.020925	0.848	0.001400	0.566004	140.860	0.308
mtDNA-CN	IDP dMRI TBSS FA Sagittal stratum R	132.750976	0.258	−0.000880	0.740045	157.752	0.063
mtDNA-CN	rfMRI connectivity (ICA100 edge 1203)	125.577619	0.569	−0.003229	0.172438	129.446	0.556
mtDNA-CN	rfMRI connectivity (ICA100 edge 1298)	119.134004	0.722	−0.001365	0.562847	121.705	0.704
mtDNA-CN	rfMRI connectivity (ICA100 edge 426)	88.957145	0.985	−0.000125	0.959276	137.129	0.398
mtDNA-CN	rfMRI connectivity (ICA100 edge 55)	120.621412	0.544	−0.002317	0.360930	147.843	0.159
mtDNA-CN	rfMRI connectivity (ICA25 edge 90)	136.907247	0.300	−0.004663	0.056686	143.311	0.234
mtDNA-CN	IDP dMRI ProbtrackX L2 ptr r	110.688765	0.760	0.002349	0.357743	139.115	0.323
mtDNA-CN	rfMRI connectivity (ICA100 edge 1215)	91.253649	0.980	0.002162	0.378359	129.013	0.570
mtDNA-CN	rfMRI connectivity (ICA100 edge 138)	115.454154	0.696	−0.000537	0.821178	142.997	0.244
mtDNA-CN	rfMRI connectivity (ICA100 edge 710)	71.041466	0.999	−0.001299	0.599784	104.390	0.950
mtDNA-CN	rfMRI connectivity (ICA100 edge 553)	109.804532	0.797	−0.001589	0.528592	133.012	0.472
mtDNA-CN	rfMRI connectivity (ICA100 edge 1284)	138.236427	0.273	−0.000635	0.794686	141.050	0.291
mtDNA-CN	rfMRI connectivity (ICA100 edge 316)	122.115284	0.654	−0.001845	0.434557	124.416	0.675
mtDNA-CN	rfMRI connectivity (ICA100 edge 717)	124.817944	0.437	−0.000719	0.781618	145.950	0.219
mtDNA-CN	IDP dMRI TBSS FA Superior fronto-occipital fasciculus L	124.116451	0.455	0.002723	0.256468	159.731	0.058
mtDNA-CN	rfMRI connectivity (ICA100 edge 379)	96.155109	0.946	0.001209	0.616542	132.585	0.466
mtDNA-CN	IDP dMRI TBSS L2 Sagittal stratum R	155.635935	0.055	0.002908	0.263483	160.216	0.042
mtDNA-CN	IDP dMRI TBSS L2 Posterior thalamic radiation R	115.713983	0.667	−0.000005	0.998468	147.484	0.170

Notes: a. The Q value tests for heterogeneity among SNPs. A significant Q value ($P < 0.05$) suggests potential pleiotropic effects that may bias the analysis, while a non-significant Q value supports consistent causal effects without substantial pleiotropy.

b. RSSobs represents "Residual Sum of Squares observed" in the MR-PRESSO analysis.

c. In MR-PRESSO, the *Global Test P*-value evaluates horizontal pleiotropy across all instruments. A significant P-value ($P < 0.05$) indicates pleiotropy, suggesting alternative pathways influencing the outcome, while a non-significant P-value supports the causal estimate's validity.

https://doi.org/10.2147/NSS.S487782

The Causal Effect of BIPs on SA

The IVs associated with the BIPs, all of which were included in the step 2 analysis, along with their corresponding F-statistics (all exceeding 10), were detailed in Tables S12-17. Using a threshold of $P < 5\times10^{-8}$ in this section would result in an insufficient number of IVs.

We investigated the causal relationships between the 6 BIPs. After BH correction, two BIPs were found to remain significantly associated with SA (Table S18), which exhibited no evidence of pleiotropy. A significant negative association was observed between "IDP dMRI TBSS L2 posterior thalamic radiation R" and SA risk (OR = 0.920, 95% CI [0.876:0.966], $P = 8.39 \times 10^{-4}$) (Figures 4B and 5B), indicating that individuals with fewer low L2 signals in the right posterior thalamic radiation had a higher SA prevalence. No evidence of horizontal pleiotropy (Egger intercept = 2.398×10^{-3}, P = 0.590; RSSobs = 56.514, Global Test $P = 0.095$) was detected for this phenotype (Figure 5A), nor was there evidence of heterogeneity (Q_pval = 0.158, $I^2 = 17.0\%$). The leave-one-out analysis indicated that no single SNP had an excessive influence on the overall causal effect estimate (Figure 5C), and the distribution of the funnel plot was largely symmetrical (Figure 5D). BFMR analysis for the BIP yielded similar results (estimate = −0.068 [−0.117, −0.019], Rhat = 1.003, $P = 6.53 \times 10^{-3}$). Additionally, "IDP dMRI TBSS FA sagittal stratum R" exhibited a significant positive association with SA risk (OR = 1.080, 95% CI [1.034:1.129], $P = 6.09\times10^{-4}$) (Figures 4B and 5F), suggesting that individuals with a higher frequency of low FA signals in the right sagittal stratum had increased SA prevalence. Similarly, no evidence of horizontal pleiotropy (Egger intercept = 2.76×10^{-3}, P = 0.466; *RSSobs = 60.081*, Global Test *P = 0.094*) was detected for this phenotype (Figure 5E), nor was there evidence of high heterogeneity (Q_pval = 0.669, $I^2 = 0.0\%$). The leave-one-out analysis and funnel plot also did not detect any outlier SNPs (Figure 5G-H). BFMR analysis demonstrated similar results (estimate = 0.062 [0.011, 0.114], Rhat = 1.011, $P = 1.71\times 10^{-2}$). Recalculating after excluding marginal SNPs with F-statistics close to 10 did not alter the nature of the results (Tables S19-20).

Mediated Proportion Analysis

We observed that "IDP dMRI TBSS L2 posterior thalamic radiation R" and "IDP dMRI TBSS FA in the sagittal stratum R" had contrasting associations with SA risk, with the former showing a significant negative association and the latter a significant positive association. The mediation proportion for the former was 11.37% (95% CI [0.25%, 22.49%], $P = 0.0450$), and for the latter, it was 12.79% (95% CI [1.08%, 24.49%], $P = 0.03228$) (Figure 6). All the statistical tests were two-sided. Differences were considered statistically significant at $P < 0.05$.

Discussion

In this study, we utilised bidirectional two-sample and two-step MR analyses to explore the causal relationship between mtDNA-CN and SA, as well as potential mediators. The results indicated a unidirectional causal relationship between genetically predicted mtDNA-CN and SA, with mtDNA-CN exhibiting a negative causality on SA. Additionally, we identified certain BIPs related to white matter microstructure and mean fractional anisotropy measurements as potential mediating components in this process.

This novel finding complements the existing literature on SA pathophysiology. SA is known to be characterized by upper airway obstruction, central neural regulation impairments, oxidative stress, inflammation, and systemic metabolic dysregulation due to intermittent hypoxia.[34,46–48] Among the IVs for mtDNA-CN, some SNPs have been previously associated with pathophysiological features of SA. For example, rs74874677, which regulates the *DGUOK* gene, directly impacts mitochondrial function.[49] A recent proteome-wide association study (PWAS) demonstrated that DGUOK abundance in the brain correlates with SA risk, suggesting a mitochondrial role in SA pathophysiology.[50] Additionally, rs10455872 is directly associated with lipoprotein levels,[51] rs342293 with mean platelet volume,[52] and rs4895441 with red blood cell parameters,[53] indicating potential links to metabolic and hematologic pathways involved in SA. However, further genetic analyses, such as colocalization with GTEx or eQTL data and cross-trait genomic analyses,[54] are needed to validate these associations and clarify their potential as therapeutic targets.

However, the biological mechanisms underlying mtDNA-CN are intricate, and its role as a biomarker varies across different disease contexts, necessitating an examination of its direct causal effects on diseases. Observational studies have

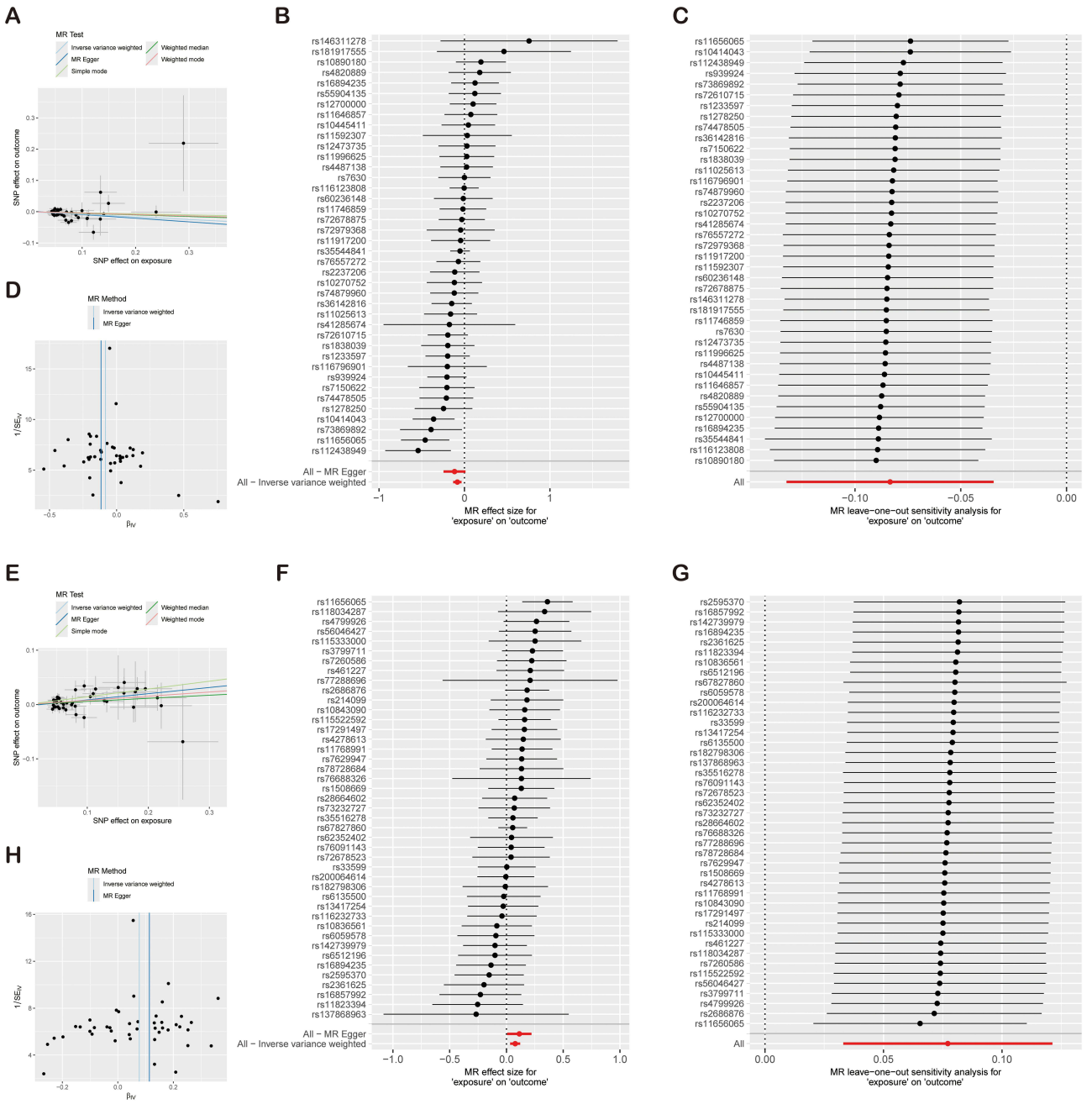

Figure 5 Forward MR analysis of the forward relationship between two BIPs identified in Step 2 of the mediation analysis and SA. (**A, E**) Scatter plots displayed the intercepts and directions; (**B, F**) Forest plots presented the effects of each SNP and the directions from MR-Egger and IVW; (**C, G**) Leave-one-out analyses assessed the robustness of the results; (**D, H**) Funnel plots evaluated the potential presence of pleiotropy. (**A–D**) represent the causal relationship between "IDP dMRI TBSS L2 posterior thalamic radiation R" and SA, while (**E–H**) represent the causal relationship between "IDP dMRI TBSS FA sagittal stratum R" and SA.

shown that individuals with lower mtDNA-CN are at greater risk for age-related complex diseases, such as coronary artery disease, sudden cardiac death, and neurodegenerative disorders.[29,55,56] In contrast, elevated levels of mtDNA (or its proportion) are closely linked to tumours.[57] Moreover, in mtDNA depletion syndromes, rare defects in nuclear genes that regulate mtDNA lead to mtDNA-CN deficiencies, resulting in brain developmental disorders.[58] Beyond these rare monogenic syndromes, the role of common genetic variations in regulating mtDNA-CN remains a vibrant area of research.[59,60] The strong confounding effects of blood cell composition and the significant differences in mtDNA-CN across various tissues and cell states further complicate the interpretation of the epidemiological associations between

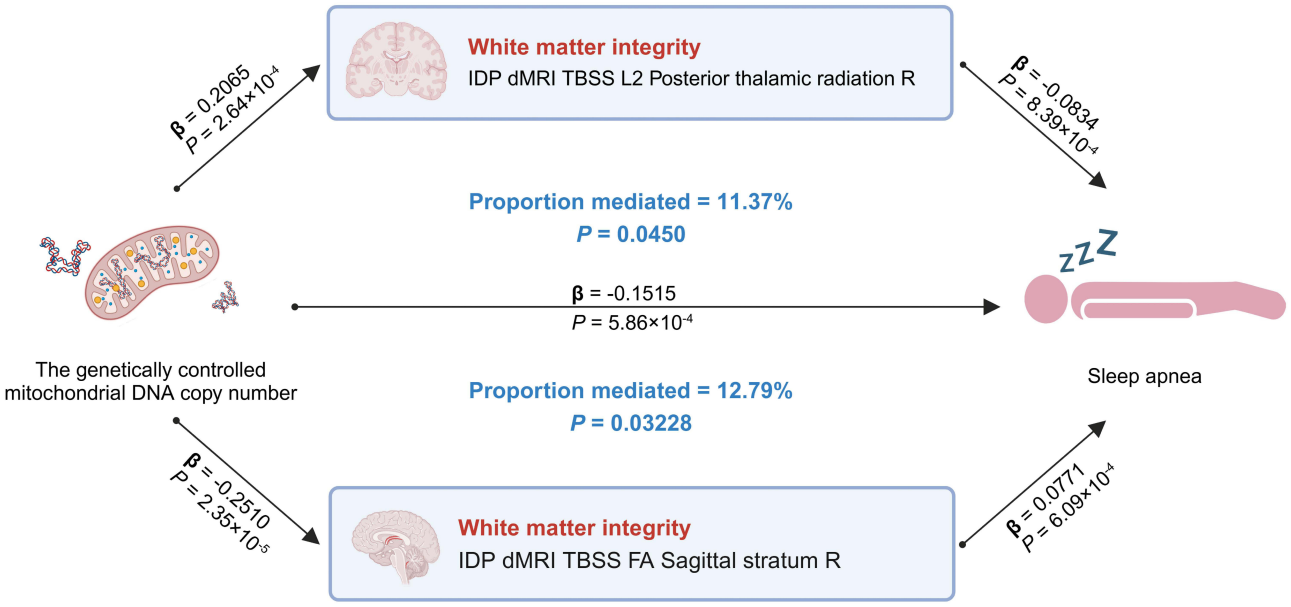

Figure 6 Potential causal evidence and mediation proportion analysis from the two-step analysis between mtDNA-CN, BIPs, and SA.

blood mtDNA-CN and disease risk.[29] Therefore, elucidating the genetic determinants of blood mtDNA-CN could enhance our understanding of the etiological processes reflected by this relatively obscure mitochondrial biomarker.

Based on the relationships among blood mtDNA-CN, platelets and immune inflammation, the potential mechanism underlying the negative causal relationship between mtDNA-CN and SA observed in this study can be partially supported. Increased mtDNA content may be associated with increased platelet counts and decreased leukocyte counts.[61,62] Tian S. et al reported that children with SA had increased platelet counts, which correlated with the severity of SA.[63] The systemic immune-inflammation index is positively associated with OSA symptoms and daytime sleepiness, and these symptoms are accompanied by greater telomere attrition in leukocytes and shorter lifespans.[64–66] Interestingly, our reverse MR analysis did not reveal a direct causal effect of SA on mtDNA-CN. However, small clinical studies have indicated poor sleep quality is associated with reduced mtDNA-CN.[67,68] These results may conflict with our findings. However, SA and poor sleep quality are not synonymous. Considering the complexity influencing blood mtDNA-CN levels, we further employed Bayesian MR analysis to maintain low Type I error rates in high heterogeneity and pleiotropy.[42] Therefore, even if there is some weak heterogeneity in the MR analysis results, this causal relationship remains valid. Interestingly, our study did not support a causal relationship between SA and mtDNA-CN, despite other studies suggesting an imbalance in mitochondrial dynamics caused by SA under hypoxic conditions.[15]

Additionally, this study demonstrated that the white matter microstructure of the right thalamic radiation and sagittal stratum might mediate the causal relationship between mtDNA-CN and SA. White matter played a critical role in transmitting and integrating information, ensuring normal brain function.[69] The thalamic radiation primarily facilitated the transmission of visual and sensory signals, while the sagittal stratum served as a key pathway connecting medial and posterior brain regions. Reduced mtDNA-CN was commonly associated with increased oxidative stress, leading to axonal degeneration and subsequent white matter damage.[70] Previous studies identified a causal link between mtDNA-CN and white matter microstructure, with evidence suggesting that mitochondrial dysfunction impaired white matter by inducing inflammatory states.[71] Conversely, an increase in mtDNA-CN was linked to improved mitochondrial function, which promoted ATP production and supported the microstructural integrity of thalamic radiation and the stability of neural signal transmission.[72] Furthermore, clinical findings reported anatomical abnormalities in the thalamus and other white matter regions associated with mitochondrial DNA damage.[73] These observations suggested that an increase in mtDNA-CN provided protective effects in regions with high energy demands and vulnerability to oxidative stress, such as the thalamic radiation and sagittal stratum, by supplying additional energy and antioxidant support.

An increasing number of scientists are exploring the relationship between brain structure, sleep characteristics, and the prevalence of SA. A recent study conducted with a German cohort revealed a significant correlation between SA and elevated signal intensity in white matter.[74] Additionally, Masoumeh R. et al identified features of compromised white matter microstructure in the brains of SA patients.[75] More specifically, the thalamus participates to some extent in regulating sleep and wakefulness, which are linked to respiratory patterns; for instance, thalamic dysfunction is thought to affect sleep depth and structure, thereby indirectly influencing respiratory rhythm.[76,77] The sagittal stratum, associated with the brain's integrative and connective functions, may indirectly influence respiratory patterns by affecting cognition and wakefulness.[78,79] This aligns partially with the findings of Jung-Ick B et al.[80] Therefore, the microstructure of the posterior thalamic radiation may help reduce arousal and respiratory instability, whereas enhanced microstructure in the sagittal stratum may increase arousal and fragmented sleep, thereby exacerbating SA. However, considering that the mediation proportion of the two white matter brain regions remains between 10–20%, indicating only a modest mediating effect, their role in the causality between mtDNA-CN and SA warrants further substantiation.

Numerous reviews have examined the use of IVs and the assumptions required for their validity, particularly in estimating causal effect parameters.[81,82] To increase the number of instruments and improve causal inference feasibility in studies with limited sample sizes, we applied a lenient threshold ($P < 1\times10^{-5}$), consistent with some MR studies.[83,84] However, this approach may increase weak instrument bias and false-positive rates.[85] To mitigate these risks, we ensured that all IVs had F-statistics exceeding 10 and excluded marginal SNPs (F-statistics between 10 and 20) for further validation. The exclusion did not alter the nature of the results or introduce horizontal pleiotropy, although it occasionally led to mild heterogeneity. The impact of this heterogeneity on the results was minimal but suggested the presence of potential biological pathways. To address this, various sensitivity analyses (Cochran's Q, MR-Egger, MR-PRESSO) were employed to confirm the absence of significant heterogeneity. To further enhance reliability, we applied a Bayesian MR framework, as proposed by Andrew JG et al, which supports robust causal inference under general conditions while maintaining low Type I error rates.[42]

Our study has certain limitations. Firstly, types of apnea and hypopnea include central SA, obstructive SA and mixed SA.[2] In this study, outcome data from the FinnGen project were based on the Finnish adaptation of ICD-10 codes, ensuring validity and consistency.[30] However, the data did not distinguish between SA subtypes, which is essential for accurate prediction, diagnosis, and treatment. Secondly, the analysis is based on a European population, which may limit the generalizability of the findings to other populations, so it is necessary to conduct GWAS studies in diverse populations in the future. Thirdly, our research elucidates the role of BIPs as mediating factors; however, whether other intermediary factors exist remains unclear. Fourthly, the data on mtDNA-CN and SA are still limited, preventing us from conducting more in-depth stratified analyses based on age, sex, and blood cell proportions. Future research should conduct more comprehensive investigations to better understand the mechanisms by which mtDNA-CN influences SA.

Despite these limitations, this study has several notable strengths. First, it effectively integrates GWAS data to innovatively identify potential biomarkers influencing SA. Additionally, the presented results are not based on a single analysis method but are derived from multiple analyses, reinforcing the findings through convergence. Importantly, these findings hold promise for patient stratification and personalized treatment. For instance, variations in mtDNA-CN and white matter structure could help categorize SA patients into distinct subgroups, each with potentially different therapeutic needs. Patients with lower mtDNA-CN might benefit from antioxidant therapies targeting mitochondrial health, while those with pronounced white matter alterations might respond better to neuroprotective interventions. However, future multi-center clinical studies will further explore the associations between mitochondria, white matter, and SA, with a focus on refining patient stratification and developing tailored therapeutic approaches based on these biomarkers.

Conclusion

Our study emphasized the negative causal relationship of mtDNA-CN with SA, while no reverse causality was found. Additionally, it revealed the mediating effects and potential mechanisms of BIPs related to white matter microstructure, including "IDP dMRI TBSS L2 posterior thalamic radiation R" and "IDP dMRI TBSS FA in the sagittal stratum R".

These findings suggest that mtDNA-CN holds potential as a predictive and therapeutic target for SA. However, future studies should incorporate stratified analyses, and further clinical research is required to explore therapeutic interventions based on these findings.

Abbreviations

TBSS, Tract-based spatial statistics; BFMR, Bayesian framework-based Mendelian Randomization; BH, Benjamini–Hochberg; BIPs, Brain imaging phenotypes; CIs, Confidence intervals; dMRI, Diffusion magnetic resonance imaging; FA, Fractional anisotropy; GWAS, Genome-wide association study; IDP, Imaging-derived phenotype; IVs, Instrumental variables; IVW, Inverse variance weighted; MR, Mendelian randomisation; MR-PRESSO, Mendelian randomisation Pleiotropy RESidual Sum and Outlier; mtDNA-CN, Mitochondrial DNA copy number; RSSobs, Residual sum of squares observed; SA, Sleep apnea; SNPs, Single nucleotide polymorphisms.

Data Sharing Statement

All the data utilized in this research are accessible through the references cited and the links provided in the Acknowledgements and Supplementary Materials sections.

Ethics Approval and Consent to Participate

This study utilized publicly available summary statistics from GWAS, with necessary ethics approvals obtained by the respective investigators. Additionally, ethical approval was granted by the Institutional Review Board of Stomatology, Shandong University (Approval No. 20241008).

Acknowledgments

We are grateful to Michael C. et al (2022) for providing the mtDNA-CN data, which can be accessed through the GWAS Catalogue (https://www.ebi.ac.uk/gwas/publications/35023831). The SA data were obtained from the FinnGen database, and we would like to acknowledge the participants and investigators of the FinnGen study. Additionally, we appreciate the BIPs data provided by Stephen M. S. et al (2021), which can be accessed from BIG40 (Manhattan plots, full downloads, and a browsable interface) and the European Bioinformatics Institute under study accession numbers GCST90002426–GCST90006360 (ftp://ftp.ebi.ac.uk/pub/databases/gwas/summary_statistics/GCST90002426 to ftp://ftp.ebi.ac.uk/pub/databases/gwas/summary_statistics/GCST90006360).

Author Contributions

All authors made a significant contribution to the work reported, whether that is in the conception, study design, execution, acquisition of data, analysis and interpretation, or in all these areas; took part in drafting, revising or critically reviewing the article; gave final approval of the version to be published; have agreed on the journal to which the article has been submitted; and agree to be accountable for all aspects of the work.

Funding

This study was supported by the National Natural Science Foundation of China (No. 82370999) to Jie Guo.

Disclosure

The authors declare that they have no competing interests.

References

1. Jordan AS, McSharry DG, Malhotra A. Adult obstructive sleep apnoea. *Lancet*. 2014;383(9918):9918):736–747. doi:10.1016/S0140-6736(13)60734-5
2. Javaheri S, Barbe F, Campos-Rodriguez F, et al. Sleep apnea: types, mechanisms, and clinical cardiovascular consequences. *J Am Coll Cardiol*. 2017;69(7):841–858. doi:10.1016/j.jacc.2016.11.069
3. Benjafield AV, Ayas NT, Eastwood PR, et al. Estimation of the global prevalence and burden of obstructive sleep apnoea: a literature-based analysis. *Lancet Respir Med*. 2019;7(8):687–698. doi:10.1016/S2213-2600(19)30198-5

4. Strenth C, Wani A, Alla R, Khan S, Schneider FD, Thakur B. Obstructive sleep apnea and its cardiac implications in the United States: an age-stratified analysis between young and older adults. *J Am Heart Assoc*. 2024;13(12):e033810. doi:10.1161/JAHA.123.033810
5. Cho J, Jo S. Association of obstructive sleep apnea with risk of lung cancer: a nationwide cohort study in Korea. *Sci Rep*. 2024;14(1):12394. doi:10.1038/s41598-024-63238-x
6. Neelapu BC, Kharbanda OP, Sardana HK, et al. Craniofacial and upper airway morphology in adult obstructive sleep apnea patients: a systematic review and meta-analysis of cephalometric studies. *Sleep Med Rev*. 2017;31:79–90. doi:10.1016/j.smrv.2016.01.007
7. Aminian A, Wang L, Al Jabri A, et al. Adverse cardiovascular outcomes in patients with obstructive sleep apnea and obesity: metabolic surgery versus usual care. *J Am Coll Cardiol*. 2024;84(12):S0735–1097(24)07559–4. doi:10.1016/j.jacc.2024.06.008
8. Tábara LC, Burr SP, Frison M, et al. MTFP1 controls mitochondrial fusion to regulate inner membrane quality control and maintain mtDNA levels. *Cell*. 2024;187(14):3619–3637.e27. doi:10.1016/j.cell.2024.05.017
9. St John JC. Mitochondrial DNA copy number and replication in reprogramming and differentiation. *Semin Cell Dev Biol*. 2016;52:93–101. doi:10.1016/j.semcdb.2016.01.028
10. Xu W, Hong YS, Hu B, et al. Mitochondrial DNA copy number variation in asthma risk, severity, and exacerbations. *J Allergy Clin Immunol*. 2024. S0091-6749(24)00906-0. doi:10.1016/j.jaci.2024.08.022
11. Primiano G, Brunetti V, Vollono C, et al. Sleep-disordered breathing in adult patients with mitochondrial diseases: a cohort study. *Neurology*. 2021;96(2):e241–e249. doi:10.1212/WNL.0000000000011005
12. Kim YS, Kwak JW, Lee KE, et al. Can mitochondrial dysfunction be a predictive factor for oxidative stress in patients with obstructive sleep apnea? *Antioxid Redox Signal*. 2014;21(9):1285–1288. doi:10.1089/ars.2014.5955
13. Venkatesan D, Iyer M, Narayanasamy A, Gopalakrishnan AV, Vellingiri B. Plausible role of mitochondrial DNA copy number in neurodegeneration-a need for therapeutic approach in Parkinson's Disease (PD). *Mol Neurobiol*. 2023;60(12):6992–7008. doi:10.1007/s12035-023-03500-x
14. Petrica L, Gadalean F, Muntean DM, et al. Mitochondrial DNA and inflammation are associated with cerebral vessel remodeling and early diabetic kidney disease in patients with type 2 diabetes mellitus. *Biomolecules*. 2024;14(4):499. doi:10.3390/biom14040499
15. Wang S, Tan J, Miao Y, Zhang Q. Mitochondrial dynamics, mitophagy, and mitochondria-endoplasmic reticulum contact sites crosstalk under hypoxia. *Front Cell Dev Biol*. 2022;10:848214. doi:10.3389/fcell.2022.848214
16. Marchi NA, Daneault V, André C, et al. Altered fornix integrity is associated with sleep apnea-related hypoxemia in mild cognitive impairment. *Alzheimers Dement*. 2024;20(6):4092–4105. doi:10.1002/alz.13833
17. Lin S, Lin X, Chen S, et al. Association of MRI indexes of the perivascular space network and cognitive impairment in patients with obstructive sleep apnea. *Radiology*. 2024;311(3):e232274. doi:10.1148/radiol.232274
18. Zhang Y, Liu X, Wiggins KL, et al. Association of mitochondrial DNA copy number with brain MRI markers and cognitive function: a meta-analysis of community-based cohorts. *Neurology*. 2023;100(18):e1930–e1943. doi:10.1212/WNL.0000000000207157
19. Ashar FN, Zhang Y, Longchamps RJ, et al. Association of mitochondrial DNA copy number with cardiovascular disease. *JAMA Cardiol*. 2017;2(11):1247–1255. doi:10.1001/jamacardio.2017.3683
20. Das SC, Hjelm BE, Rollins BL, et al. Mitochondria DNA copy number, mitochondria DNA total somatic deletions, Complex I activity, synapse number, and synaptic mitochondria number are altered in schizophrenia and bipolar disorder. *Transl Psychiatry*. 2022;12(1):353. doi:10.1038/s41398-022-02127-1
21. Larsson SC, Butterworth AS, Burgess S. Mendelian randomization for cardiovascular diseases: principles and applications. *Eur Heart J*. 2023;44(47):4913–4924. doi:10.1093/eurheartj/ehad736
22. Sekula P, Del Greco MF, Pattaro C, Köttgen A. Mendelian randomization as an approach to assess causality using observational data. *J Am Soc Nephrol*. 2016;27(11):3253–3265. doi:10.1681/ASN.2016010098
23. Carter AR, Sanderson E, Hammerton G, et al. Mendelian randomisation for mediation analysis: current methods and challenges for implementation. *Eur J Epidemiol*. 2021;36(5):465–478. doi:10.1007/s10654-021-00757-1
24. Chong MR, Narula S, Morton R, et al. Mitochondrial DNA copy number as a marker and mediator of stroke prognosis: observational and Mendelian randomization analyses. *Neurology*. 2022;98(5):e470–e482. doi:10.1212/WNL.0000000000013165
25. Cai X, Liang C, Zhang M, Dong Z, Weng Y, Yu W. Mitochondrial DNA copy number and cancer risks: a comprehensive Mendelian randomization analysis. *Int, J, Cancer*. 2024;154(8):1504–1513. doi:10.1002/ijc.34833
26. Lu Y, Han L, Wang X, et al. Association between blood mitochondrial DNA copy number and mental disorders: a bidirectional two-sample Mendelian randomization study. *J Affect Disord*. 2024;366:370–378. doi:10.1016/j.jad.2024.08.162
27. Sanderson E, Glymour MM, Holmes MV, et al. Mendelian randomization. *Nat Rev Meth Primers*. 2022;2(1):6. doi:10.1038/s43586-021-00092-5
28. Skrivankova VW, Richmond RC, Woolf BAR, et al. Strengthening the reporting of observational studies in epidemiology using Mendelian randomisation (STROBE-MR): explanation and elaboration. *BMJ*. 2021:375:n2233. doi:10.1136/bmj.n2233
29. Chong M, Mohammadi-Shemirani P, Perrot N, et al. GWAS and ExWAS of blood mitochondrial DNA copy number identifies 71 loci and highlights a potential causal role in dementia. *Elife*. 2022:11:e70382. doi:10.7554/eLife.70382
30. Kurki MI, Karjalainen J, Palta P, et al. FinnGen provides genetic insights from a well-phenotyped isolated population. *Nature*. 2023;613:7944):-508–518. doi:10.1038/s41586-022-05473-8
31. Smith SM, Douaud G, Chen W, et al. An expanded set of genome-wide association studies of brain imaging phenotypes in UK Biobank. *Nat Neurosci*. 2021;24(5):737–745. doi:10.1038/s41593-021-00826-4
32. Bardutzky J, Shen Q, Henninger N, Schwab S, Duong TQ, Fisher M. Characterizing tissue fate after transient cerebral ischemia of varying duration using quantitative diffusion and perfusion imaging. *Stroke*. 2007;38(4):1336. doi:10.1161/01.STR.0000259636.26950.3b
33. Yu K, Chen XF, Guo J, et al. Assessment of bidirectional relationships between brain imaging-derived phenotypes and stroke: a Mendelian randomization study. *BMC Med*. 2023;21(1):271. doi:10.1186/s12916-023-02982-9
34. Liu X, Ma Y, Ouyang R, et al. The relationship between inflammation and neurocognitive dysfunction in obstructive sleep apnea syndrome. *J Neuroinflammation*. 2020;17(1):229. doi:10.1186/s12974-020-01905-2
35. Gray B, Tester DJ, Wong LC, et al. Noncardiac genetic predisposition in sudden infant death syndrome. *Genet Med*. 2019;21(3):641–649. doi:10.1038/s41436-018-0131-4
36. Pierce BL, Burgess S. Efficient design for Mendelian randomization studies: subsample and 2-sample instrumental variable estimators. *Am J Epidemiol*. 2013;178(7):1177–1184. doi:10.1093/aje/kwt084

37. Papadimitriou N, Dimou N, Tsilidis KK, et al. Physical activity and risks of breast and colorectal cancer: a Mendelian randomisation analysis. *Nat Commun*. 2020;11(1):597. doi:10.1038/s41467-020-14389-8
38. Burgess S, Thompson SG. CRP CHD Genetics Collaboration. Avoiding bias from weak instruments in Mendelian randomization studies. *Int J Epidemiol*. 2011;40(3):755–764. doi:10.1093/ije/dyr036
39. Bowden J, Davey Smith G, Burgess S. Mendelian randomization with invalid instruments: effect estimation and bias detection through Egger regression. *Int J Epidemiol*. 2015;44(2):512–525. doi:10.1093/ije/dyv080
40. MacKinnon DP, Lockwood CM, Hoffman JM, West SG, Sheets V. A comparison of methods to test mediation and other intervening variable effects. *Psychol Methods*. 2002;7(1):83–104. doi:10.1037/1082-989x.7.1.83
41. Li J, Yu Y, Sun Y, et al. SGLT2 inhibition, circulating metabolites, and atrial fibrillation: a Mendelian randomization study. *Cardiovasc Diabetol*. 2023;22(1):278. doi:10.1186/s12933-023-02019-8
42. Grant AJ, Burgess S. A Bayesian approach to Mendelian randomization using summary statistics in the univariable and multivariable settings with correlated pleiotropy. *Am J Hum Genet*. 2024;111(1):165–180. doi:10.1016/j.ajhg.2023.12.002
43. Liu M, Yu D, Pan Y, et al. Causal roles of lifestyle, psychosocial characteristics, and sleep status in sarcopenia: a Mendelian randomization study. *J Gerontol a Biol Sci Med Sci*. 2024;79(1):glad191. doi:10.1093/gerona/glad191
44. Verbanck M, Chen CY, Neale B, Do R. Detection of widespread horizontal pleiotropy in causal relationships inferred from Mendelian randomization between complex traits and diseases. *Nat Genet*. 2018;50(5):693–698. doi:10.1038/s41588-018-0099-7
45. Chen J, Yuan S, Fu T, et al. Gastrointestinal consequences of type 2 diabetes mellitus and impaired glycemic homeostasis: a Mendelian randomization study. *Diabetes Care*. 2023;46(4):828–835. doi:10.2337/dc22-1385
46. Hatipoğlu U, Rubinstein I. Inflammation and obstructive sleep apnea syndrome pathogenesis: a working hypothesis. *Respiration*. 2003;70(6):665–671. doi:10.1159/000075218
47. Light M, McCowen K, Malhotra A, Mesarwi OA. Sleep apnea, metabolic disease, and the cutting edge of therapy. *Metabolism*. 2018;84:94–98. doi:10.1016/j.metabol.2017.09.004
48. Kovbasyuk Z, Ramos-Cejudo J, Parekh A, et al. Obstructive sleep apnea, platelet aggregation, and cardiovascular risk. *J Am Heart Assoc*. 2024;13(15):e034079. doi:10.1161/JAHA.123.034079
49. Guo J, Duan L, He X, et al. A combined model of human iPSC-derived liver organoids and hepatocytes reveals ferroptosis in DGUOK Mutant mtDNA depletion syndrome. *Adv Sci (Weinh)*. 2021;8(10):2004680. doi:10.1002/advs.202004680
50. Gui J, Meng L, Huang D, et al. Identification of novel proteins for sleep apnea by integrating genome-wide association data and human brain proteomes. *Sleep Med*. 2024;114:92–99. doi:10.1016/j.sleep.2023.12.026
51. Olmastroni E, Gazzotti M, Averna M, et al. Lipoprotein(a) Genotype Influences the Clinical Diagnosis of Familial Hypercholesterolemia. *J Am Heart Assoc*. 2023;12(10):e029223. doi:10.1161/JAHA.122.029223
52. Miller MM, Henninger N, Słowik A. Mean platelet volume and its genetic variants relate to stroke severity and 1-year mortality. *Neurology*. 2020;95(9):e1153–e1162. doi:10.1212/WNL.0000000000010105
53. Timmer T, Tanck MWT, Huis In 't Veld EMJ, et al. Associations between single nucleotide polymorphisms and erythrocyte parameters in humans: a systematic literature review. *Mutat Res Rev Mutat Res*. 2019;779:58–67. doi:10.1016/j.mrrev.2019.01.002
54. Feng K, Yang J, Liu K. Shared genetic associations and etiology between obstructive sleep apnea and CVDs: a genome-wide cross-trait analysis and bidirectional Mendelian randomization analysis. *Eur J Prev Cardiol*. 2024;zwae347. doi:10.1093/eurjpc/zwae347
55. Cerantonio A, Citrigno L, Greco BM, et al. The role of mitochondrial copy number in neurodegenerative diseases: present insights and future directions. *Int J Mol Sci*. 2024;25(11):6062. doi:10.3390/ijms25116062
56. Tin A, Grams ME, Ashar FN, et al. Association between Mitochondrial DNA copy number in peripheral blood and incident CKD in the atherosclerosis risk in communities study. *J Am Soc Nephrol*. 2016;27(8):2467–2473. doi:10.1681/ASN.2015060661
57. Kim M, Gorelick AN, Vàzquez-García I, et al. Single-cell mtDNA dynamics in tumors is driven by coregulation of nuclear and mitochondrial genomes. *Nat Genet*. 2024;56(5):889–899. doi:10.1038/s41588-024-01724-8
58. Gorman GS, Chinnery PF, DiMauro S, et al. Mitochondrial diseases. *Nat Rev Dis Primers*. 2016;2(1):16080. doi:10.1038/nrdp.2016.80
59. Hägg S, Jylhävä J, Wang Y, Czene K, Grassmann F. Deciphering the genetic and epidemiological landscape of mitochondrial DNA abundance. *Hum Genet*. 2021;140(6):849–861. doi:10.1007/s00439-020-02249-w
60. Guyatt AL, Brennan RR, Burrows K, et al. A genome-wide association study of mitochondrial DNA copy number in two population-based cohorts. *Hum Genomics*. 2019;13(1):6. doi:10.1186/s40246-018-0190-2
61. Picard M. Blood mitochondrial DNA copy number: what are we counting? *Mitochondrion*. 2021;60:1–11. doi:10.1016/j.mito.2021.06.010
62. Knez J, Winckelmans E, Plusquin M, et al. Correlates of peripheral blood mitochondrial DNA content in a general population. *Am J Epidemiol*. 2016;183(2):138–146. doi:10.1093/aje/kwv175
63. Shen T, Wang J, Li L, et al. Changes in platelet count and coagulation parameters in children with obstructive sleep apnea. *Sleep Breath*. 2022;26(2):871–878. doi:10.1007/s11325-021-02443-8
64. Kadier K, Dilixiati D, Ainiwaer A, et al. Analysis of the relationship between sleep-related disorder and systemic immune-inflammation index in the US population. *BMC Psychiatry*. 2023;23(1):773. doi:10.1186/s12888-023-05286-7
65. Zota IM, Adam CA, Marcu DTM, et al. CPAP influence on readily available inflammatory markers in OSA-A pilot study. *Int J Mol Sci*. 2022;23(20):12431. doi:10.3390/ijms232012431
66. Carroll JE, Irwin MR, Seeman TE, et al. Obstructive sleep apnea, nighttime arousals, and leukocyte telomere length: the multi-ethnic study of atherosclerosis. *Sleep*. 2019;42(7):zsz089. doi:10.1093/sleep/zsz089
67. Maqsood M, Ali S, Ahmed S, Feroz S. Effect of Sleep Quality on Mitochondrial DNA Copy Number in Eveningness Chronotypes. *J Coll Physicians Surg Pak*. 2024;34(1):73–77. doi:10.29271/jcpsp.2024.01.73
68. Han S, Kim DK, Jun SE, Kim N. Association of sleep quality and mitochondrial DNA copy number in healthy middle-aged adults. *Sleep Med*. 2024;113:19–24. doi:10.1016/j.sleep.2023.11.011
69. Lebel C, Deoni S. The development of brain white matter microstructure. *Neuroimage*. 2018;182:207–218. doi:10.1016/j.neuroimage.2017.12.097
70. Nguyen H, Zerimech S, Baltan S. Astrocyte mitochondria in white-matter injury. *Neurochem Res*. 2021;46(10):2696–2714. doi:10.1007/s11064-021-03239-8

71. Zhou XY, Thai M, Roediger D, et al. Mitochondrial health, NLRP3 inflammasome activation, and white matter integrity in adolescent mood disorders: a pilot study. *J Affect Disord*. 2023;340:149–159. doi:10.1016/j.jad.2023.08.039
72. Zhao M, Su HZ, Zeng YH, et al. Loss of function of CMPK2 causes mitochondria deficiency and brain calcification. *Cell Discov*. 2022;8(1):128. doi:10.1038/s41421-022-00475-2
73. Yamadori I, Kurose A, Kobayashi S, Ohmori M, Imai T. Brain lesions of the Leigh-type distribution associated with a mitochondriopathy of Pearson's syndrome: light and electron microscopic study. *Acta Neuropathol*. 1992;84(3):337–341. doi:10.1007/BF00227830
74. Zacharias HU, Weihs A, Habes M, et al. Association between obstructive sleep apnea and brain white matter hyperintensities in a population-based cohort in Germany. *JAMA Network Open*. 2021;4(10):e2128225. doi:10.1001/jamanetworkopen.2021.28225
75. Rostampour M, Noori K, Heidari M, et al. White matter alterations in patients with obstructive sleep apnea: a systematic review of diffusion MRI studies. *Sleep Med*. 2020;75:236–245. doi:10.1016/j.sleep.2020.06.024
76. Bastuji H, Daoud M, Magnin M, Garcia-Larrea L. REM sleep remains paradoxical: sub-states determined by thalamo-cortical and cortico-cortical functional connectivity. *J Physiol*. 2024;602(20):5269–5287. doi:10.1113/JP286074
77. Shin S, Seok JW, Kim K, Kim J, Nam HY, Pak K. Poor sleep quality is associated with decreased regional brain glucose metabolism in healthy middle-aged adults. *Neuroimage*. 2024;298:120814. doi:10.1016/j.neuroimage.2024.120814
78. Xiong Y, Zhou XJ, Nisi RA, et al. Brain white matter changes in CPAP-treated obstructive sleep apnea patients with residual sleepiness. *J Magn Reson Imaging*. 2017;45(5):1371–1378. doi:10.1002/jmri.25463
79. Abdelhack M, Zhukovsky P, Milic M, et al. Opposing brain signatures of sleep in task-based and resting-state conditions. *Nat Commun*. 2023;14(1):7927. doi:10.1038/s41467-023-43737-7
80. Byun JI, Jahng GH, Ryu CW, et al. Altered intrinsic brain functional network dynamics in moderate-to-severe obstructive sleep apnea. *Sleep Med*. 2023;101:550–557. doi:10.1016/j.sleep.2022.12.003
81. Burgess S, Small DS, Thompson SG. A review of instrumental variable estimators for Mendelian randomization. *Stat Methods Med Res*. 2017;26(5):2333–2355. doi:10.1177/0962280215597579
82. Glymour MM, Tchetgen EJT, Robins JM. Credible Mendelian randomization studies: approaches for evaluating the instrumental variable assumptions. *American Journal of Epidemiology*. 2012;175(4):332. doi:10.1093/aje/kwr323
83. Sanna S, van Zuydam NR, Mahajan A, et al. Causal relationships among the gut microbiome, short-chain fatty acids and metabolic diseases. *Nat Genet*. 2019;51(4):600–605. doi:10.1038/s41588-019-0350-x
84. Liu L, He G, Yu R, et al. Causal relationships between gut microbiome and obstructive sleep apnea: a bi-directional Mendelian randomization. *Front Microbiol*. 2024;15:1410624. doi:10.3389/fmicb.2024.1410624
85. Davies NM, Holmes MV, Davey Smith G. Reading Mendelian randomisation studies: a guide, glossary, and checklist for clinicians. *BMJ*. 2018;362:k601. doi:10.1136/bmj.k601